A lithographic approach for quantum dot-photonic crystal nanocavity coupling in dilute nitrides

G. Pettinari[a,*], A. Gerardino[a], L. Businaro[a], A. Polimeni[b], M. Capizzi[b], M. Hopkinson[c], S. Rubini[d], F. Biccari[e], F. Intonti[e], A. Vinattieri[e], M. Gurioli[e], M. Felici[b]

[a] National Research Council, Institute for Photonics and Nanotechnologies (IFN-CNR), Via Cineto Romano 42, 00156, Rome, Italy
[b] Dipartimento di Fisica, Sapienza Università di Roma, P.le A. Moro 5, 00185, Roma, Italy
[c] Department of Electronic and Electrical Engineering, University of Sheffield, 3 Solly Street, Sheffield S1 4DE, United Kingdom
[d] IOM-CNR Laboratorio TASC, S. S. 14, Km 163.5, 34149 Trieste, Italy
[e] LENS and Dipartimento di Fisica,Università di Firenze, via G. Sansone 1, 50019, Sesto Fiorentino (FI), Italy

We report on a novel lithographic approach for the fabrication of integrated quantum dot (QD)-photonic crystal (PhC) nanocavity systems. We exploit unique hydrogen's ability to tailor the band gap energy of dilute nitride semiconductors to fabricate site-controlled QDs via a spatially selective hydrogenation at the nanometer-scale. A deterministic integration of the realized site-controlled QDs with PhC nanocavities is provided by the inherent realignment precision (~20 nm) of the electron beam lithography system used for the fabrication of both QDs and PhC cavities. A detailed description of the fabrication steps leading to the realization of integrated QD-PhC cavity systems is provided, together with the experimental evidence of a weak coupling effect between the single-photon emitter and the PhC cavity.

Keywords: site-controlled QDs, photonic crystal structures, dilute nitrides, hydrogen in semiconductors.

1. Introduction

The fabrication of integrated quantum dot (QD)-optical nanocavity systems is a pivotal step for the realization of innovative nanophotonic applications and devices, such as quantum computing, quantum key distribution, nano-lasers, efficient single-photon emitters etc., as well as for fundamental studies on cavity quantum electrodynamics (cavity-QED) [1,2]. One of the main strategies for integrating a QD into an optical cavity is the fabrication of a photonic crystal (PhC) cavity around a selected QD [3]. The main drawback of this approach is the difficulty of obtaining the isolation of a single high-quality QD and of deterministically matching it both spatially and spectrally with the PhC cavity modes.

In the past, we have demonstrated the possibility of fabricating isolated site-controlled QDs by means of a spatially selective hydrogen incorporation in Ga(AsN)/GaAs heterostructures [4]. The ability of such site-controlled QDs to act as single photon emitters has also been reported [5]. Indeed, the formation of stable N-H complexes removes the effects nitrogen has on the optical, structural, and electronic properties of the host materials [6,7]. In particular, H atom binding to N atoms in Ga(AsN) leads to an increase in the band gap energy of the N-containing material (~1.33 eV at T = 5 K for [N] = 1%) up to the value it has in GaAs (1.52 eV at T = 5 K). The ability to tailor the alloy band gap energy by hydrogen incorporation can be engineered by patterning the sample's surface with H-opaque masks prior to the hydrogenation process, to attain a modulation of the band gap energy in the growth plane. This band gap spatial modulation can then be pushed down to the nanoscale, tuning the carrier-confining potential to fabricate site-controlled, dilute nitride-based QDs in a GaAs-like matrix.

Here, we demonstrate the possibility of integrating deterministically such site-controlled QDs into photonic crystal nanocavities. A fabrication approach based on electron beam lithography (EBL) has been developed to get both spatial and spectral deterministic couplings between the quantum emitter and the PhC cavity. The detailed fabrication process is described in the following sections; moreover, the evidence of a weak coupling between the QD and the cavity is provided via the experiment observation of the Purcell effect [8], namely, the enhancement of the spontaneous emission rate of an emitter on resonance with a mode of an optical cavity.

2. Fabrication process

Integrated QD-PhC cavity systems were fabricated out of a heterostructure grown by molecular beam epitaxy (MBE) on top of a (001) GaAs substrate. The heterostructure consists of a 6 nm-thick Ga(AsN)/GaAs quantum well (QW) ([N] ~ 1.1%) sandwiched between a 130 nm-thick GaAs buffer layer and a 30 nm-thick GaAs capping layer, all grown on top of a 1500 nm-thick (AlGa)As sacrificial layer ([Al] = 70%). The fabrication of both the site-controlled QD and PhC cavity was obtained by means of EBL (Vistec EPBG 5HR system working at 100 kV) and thin-film techniques (see sections 2.1 and 2.2); whilst the deterministic spatial and spectral coupling between the emitter and the cavity was achieved exploiting the inherent realignment precision

(~20 nm) and spatial resolution (~4 nm) of the EBL system itself (see sections 2.3 and 3).

2.1 Site-controlled QD fabrication

Figure 1 shows a schematic representation of the site-controlled dilute nitride QD fabrication process. An isolated H-opaque circular mask is first patterned by EBL on the sample's surface. As described in details in Refs. [4,7], the hydrogenation of a dilute nitride-based heterostructure covered with a H-opaque mask results in a spatially controlled diffusion of hydrogen inside the sample, and, eventually, in a well-defined spatial region of Ga(AsN) material completely surrounded by GaAs-like material –i.e., GaAs or fully-hydrogenated Ga(AsN), having the latter the same band gap energy of GaAs. Due to partial H diffusion beneath the mask [4,7], the actual size of the Ga(AsN) region can be smaller than the physical size of the mask; see Fig. 1b. For the integration with PhC cavities, arrays of isolated (35 µm spacing) circular masks of different diameter (ranging from 80 nm to 500 nm) were patterned by EBL with a negative-tone HSQ (hydrogen silsesquioxane) resist. The sample was then irradiated with hydrogen ions by means of a Kaufman source [9]. The ion-beam kinetic energy was set to a low value (100 eV) in order to minimize sample damage, whilst the sample was kept at a temperature of 190 °C for the entire duration of the irradiation process, to allow H-diffusion inside the sample while maintaining an extremely sharp diffusion profile (hydrogen forefront less than 5 nm/decade; see Ref. [7]). Different hydrogen doses were investigated, in order to reach a full passivation of the open region and a well-defined Ga(AsN) dot beneath the mask.

The optimal conditions to get an array of identical Ga(AsN) QDs with a single, sharp (~150 µeV broad) emission line at about 1.31 eV and an energy distribution of ~30 meV –i.e., of the order of the Ga(AsN) QW linewidth they originate from– were obtained for a mask diameter size of 160 nm and a total hydrogen dose of 9×10^{16} ions/cm^2.

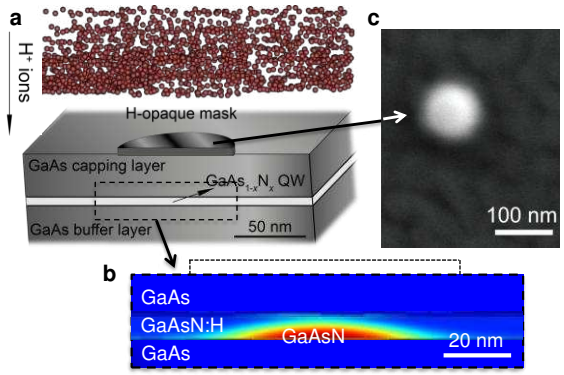

FIG. 1. Schematic representation of the dilute nitride QD fabrication process: The hydrogen irradiation of a Ga(AsN)/GaAs heterostructure patterned with a nanometer-size H-opaque circular mask (a) results in a nanometer region of Ga(AsN) embedded in a GaAs or Ga(AsN):H matrix (b). (c) SEM image of a HSQ H-opaque mask (80 nm in diameter) patterned by electron beam lithography.

2.2 PhC cavity fabrication

We fabricated a series of PhC L_3 defect cavities (namely, optical cavities generated in a PhC membrane by removing three air-holes in a line from the otherwise periodic hexagonal lattice; see Fig. 2e) with the same filling-ratio r/a = 0.29 (being r and a the radius of the air-holes and the PhC lattice constant, respectively) and different value of lattice constant (ranging from 230 nm to 262 nm). The PhC design parameters were defined by FDTD simulations with the aim to get the fundamental cavity mode (CM) at about the same energy of the QD ground state transition (E_X ~ 1.31 eV).

The PhC fabrication process is sketched in Fig. 2. The sample (Fig. 2a) is first covered with a thin layer (~400 nm) of positive-tone electron-beam resist (ZEP520A), which is baked on a hot-plate at 180 °C for two minutes before EBL exposure. The desired pattern is then exposed with an electron dose of 900 µC/cm^2 and developed at 20 °C in a mixture of MIBK:IPA (1:1) for

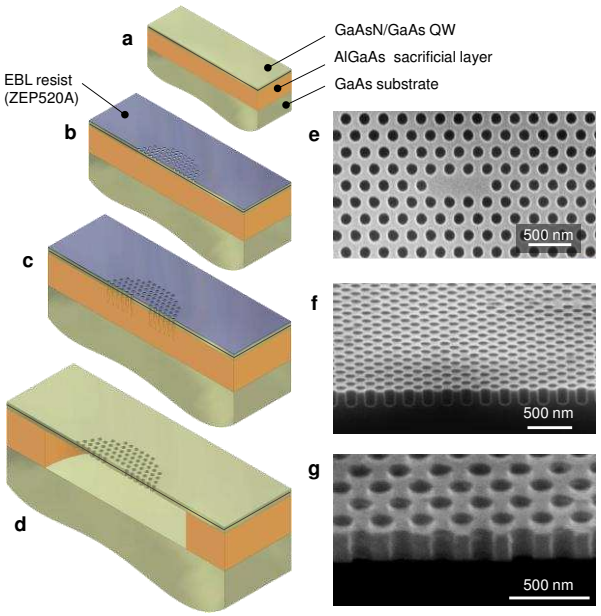

FIG. 2. Schematic representation of the photonic crystal cavity fabrication process: The Ga(AsN)/GaAs heterostructure grown on top of an (AlGa)As sacrificial layer (a) is covered with an EBL positive-tone resist (ZEP520A) and patterned by EBL with the required PhC design (b), the PhC design is then transferred into the Ga(AsN)/GaAs layer by means of a Cl-based dry etching (c), finally, the GaAs membrane is released by a HF wet etching of the (AlGa)As sacrificial layer (d). SEM images of the sample at the end of the dry etching process (e: tilted at 0° and f: tilted at 75°) and after the release of the membrane (g: tilted at 60°) are shown.

60 seconds (Fig. 2b). The PhC design is then etched into the Ga(AsN)/GaAs membrane by means of a Cl-based reactive ion etching (Fig. 2c). Etching steps with a BCl_3:Cl_2:Ar (39:2.6:5.6 sccm) gas mixture at a pressure of 9.5 mTorr excited by a radio-frequency power of 90 W were used, alternated with oxygen plasma cleaning steps. This condition results in a GaAs etching rate of about 17 nm/min (as measured directly on the holes of the PhC pattern, see Fig. 2f) and in a resist etching rate of about 25 nm/min. The electron-beam resist can be successfully used as a mask during the dry etching process, without the need of any extra processing steps. The choice of a BCl_3:Cl_2:Ar mixture for the PhC etching results in a highly anisotropic etching and, eventually, in a highly vertical sidewalls in the PhC air-holes (see Figs. 2f and 2g). Indeed, Cl_2 guarantees an efficient chemical etching of GaAs, whilst BCl_3 provides a good sidewall surface inhibition and Ar spattering removes the products of the reaction from the bottom of the holes, keeping the etching process active and homogenous [10,11,12].

At the end of the dry etching the residual resist is removed by a wet etching in hot anisole. The membrane containing the PhC structure is finally released by wet etching of the (AlGa)As sacrificial layer with a 5% solution of hydrofluoric acid (Figs. 2d and 2g), in order to provide vertical optical isolation.

2.3 Integrated QD-PhC cavity system fabrication

The deterministic integration of the site-controlled QDs with the PhC cavities described in the previous sections relies on the realignment precision between successive steps (~20 nm) of the EBL system. An overview of the entire fabrication flow is given in Fig. 3. The first step consists in patterning the sample's surface with Cr/Au markers, to be used as a spatial reference for successive realignments in the lithographic process. Then, the site-controlled QDs are fabricated as described in section 2.1. After the formation of the QD, the HSQ mask is removed by alternating reactive ion etching steps using a CHF_3:O_2 (120:10 sccm) gas mixture at a pressure of 55 mTorr excited by a radio-frequency power of 100 W with oxygen plasma cleaning steps. Finally, the PhC cavities are fabricated on the sample as described in section 2.2, with cavity centered to the isolated QD emitter.

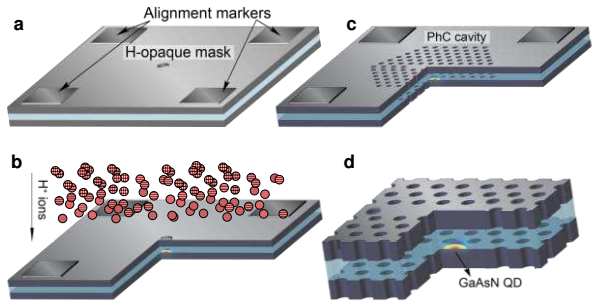

FIG. 3. Sketch of the processing steps leading to the fabrication of an integrated QD-PhC cavity system: A series of alignment markers and a H-opaque mask are first realized on the surface of a Ga(AsN)/GaAs heterostructure (a), the sample is then irradiated with atomic hydrogen resulting in a Ga(AsN) QD beneath the mask (b; see also Fig. 1). By using the alignment markers as a spatial reference, a photonic crystal cavity is realized centered with the QD (c; see also Fig. 2). This lithographic approach allows a spatial coupling uncertainty between the QD and the PhC cavity of about 20 nm, limited only by the realignment precision of the EBL system used (d).

3. Results and Discussion

The optical properties of the integrated QD-PhC cavity systems were characterized by autocorrelation and temperature-dependent photoluminescence (PL) spectroscopy measurements.

As regards the properties of the site-controlled QDs, these have been already investigated in details in previous publications [4,5,7]. Here, we confirm the ability of the fabricated QDs to act as a single photon emitter also when integrated into a photonic crystal cavity, which is a crucial property for the successful employment of these systems in future applications. Evidence of such a non-classical behavior of light is given by the observation of a strong antibunching in the autocorrelation histogram of the QD exciton emission line. Figure 4a displays a typical photon-correlation measurement acquired on a QD (mask diameter 160 nm) integrated into a PhC L_3 defect cavity (r/a = 0.29, a = 255 nm). The QD emission was excited by a pulsed Ti:Sapphire laser (80 MHz repetition rate) frequency-doubled with a BBO non-linear crystal (excitation wavelength = 390 nm) focused trough a 100× microscope objective with 0.7 numerical aperture up to a power density on the sample of 30 W/cm^2. The emission was analyzed by means of an Hanbury Brown and Twiss (HBT) setup (time resolution ~300 ps) centred at the wavelength of the QD ground state transition (E_X = 1.314 eV).

The statistics of the photons emitted by the recombination of neutral excitons in a single QD can be described by the second-order autocorrelation function [13]

$$g^{(2)}(\tau) = \frac{\langle I(t)I(t+\tau)\rangle}{\langle I(t)\rangle^2}, \quad (1)$$

where I(t) and I($t + \tau$) are the light intensities at the time t and after a time delay τ, respectively. The value of the autocorrelation function at zero delay gives the number (N) of emitted photons at a given time [13]:

$$g^{(2)}(0) = 1 - \frac{1}{N}. \quad (2)$$

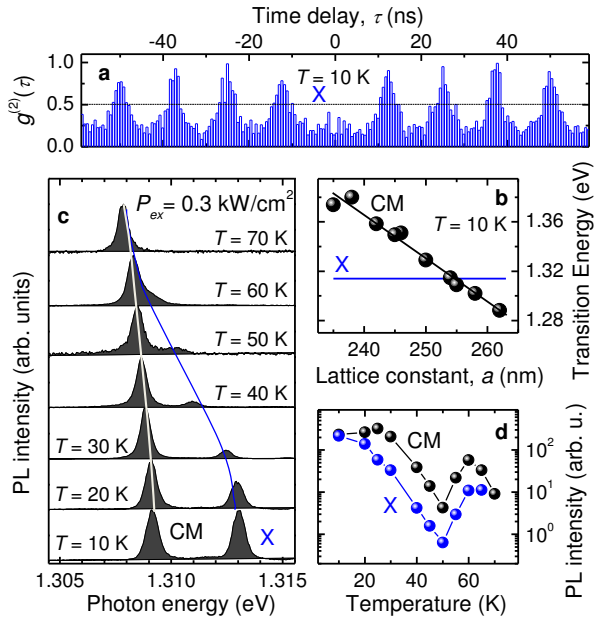

FIG. 4. Optical characterization of the integrated QD-PhC system: (a) Second-order autocorrelation of the exciton ground state transition (X) of the site-controlled QD (mask diameter 160 nm). Note the $g^{(2)}(0) < 0.5$, providing evidence of the single-photon emission regime. (b) Lithographic tuning of the cavity mode (CM) energy of a PhC L_3 defect cavity (r/a = 0.29) by varying the lattice constant value. Note the pretty good linear dependence of the CM with a dE_{CM}/da ~3.5 meV/nm. The emission energy of the QD transition X is also reported for comparison. (c) Peak normalized photoluminescence (PL) spectra showing the temperature-dependent CM-QD detuning. (d) The increase of integrated PL intensity for both the CM and the X transitions for decreasing energy detuning (i.e., for increasing temperature above ~50 K) is a result of the QD-PhC cavity coupling effect (i.e., Purcell effect).

For a pure single photon source (N = 1), a value of $g^{(2)}(0) = 0$ is expected; however, the presence of a single quantum emitter is commonly confirmed by the observation of a $g^{(2)}(0)$ less than 0.5 (i.e., N < 2). In our case, we observe a strong suppression of the autocorrelation peak at zero delay time, with a value of $g^{(2)}(0) < 0.5$ (and close to the background level) that proves the single photon emission from our QDs. The quite high level (~0.25) of background signal in our measurements is most likely due to carrier recapture phenomena [14,15] associated with the relatively high power density (30 W/cm^2) we used. The excitation conditions employed in this work, indeed, were chosen to obtain fast autocorrelation measurements (collection time less than 1 hour), while maintaining the background level reasonably below the critical value of 0.5.

As regards the PhC cavities, a lithographic tuning of the cavity mode (CM) energy –i.e., a fine variation of the PhC lattice constant a– was performed to match the emission energy of the QD; see Fig. 4b. A first coarse spectral matching between the CM and the QD emissions was reached with a PhC L_3 defect cavity with a = 255 nm, for which a satisfactory quality factor of ~2500 was obtained, close to the theoretical value (3200) of a perfect GaAs PhC L_3 cavity working at ~950 nm [16]. The small energy detuning (~4 meV) between the CM and QD peaks at T = 10 K was then reduced by increasing the sample temperature; see Fig. 4c. Indeed, by increasing the temperature, the QD emission undergoes a sizable energy redshift, whilst the PhC CM energy is only slightly perturbed, following the weak temperature variation of the refractive index of the cavity: 24 μeV/K [17]. This brings the two transitions on resonance for T ~ 60 K. An analysis of the PL intensity of the CM and QD ground state transitions, performed by fitting the experimental spectra using a Gaussian for the QD peak and a Lorentzian for the CM one, provides an evidence of the Purcell effect on our integrated QD-PhC cavity systems. Indeed, the PL intensity of both CM and QD transitions initially decreases by increasing the temperature, as a result of the thermal activation of non-radiative channels [18], then, for high temperature (T > 50 K) (i.e., small energy detuning: < 1.5 meV), both transitions gain intensity, reflecting the enhancement of the spontaneous emission rate of the emitter, which starts to interact with the optical cavity. A more detailed study of this effect and of the realized integrated systems is in progress and will be reported elsewhere [19].

4. Conclusions

In summary, we demonstrated a novel lithographic approach allowing a deterministic spatial and spectral matching between a site-controlled single-photon emitter (i.e., a dilute nitride-based QD) and a photonic crystal nanocavity. In particular, the high spatial resolution made available by electron beam lithography guarantees the spatial matching between the emitter and the cavity, whilst a good spectral matching can be achieved by a fine lithographic tuning of the PhC lattice constant (i.e., cavity mode energy). A detailed description of the entire fabrication process is provided in the present work, and experimental evidence of weak coupling (i.e., Purcell effect) is reported for a QD emitting at ~950 nm integrated in a PhC L_3 defect cavity (r/a = 0.29, a = 255 nm) with a quality factor of 2500. It is worth mentioning that the nanofabrication method presented here could be extended to obtain integrated systems working at wavelengths of interest for telecommunication applications simply by using samples with larger nitrogen content ([N] ~ 4%) or, alternatively, by using an (InGa)(AsN) quantum well [20] instead of a Ga(AsN) one.

Acknowledgments

The authors acknowledge S. Birindelli (Eindhoven University of Technology) for useful discussions at the early stage of the project and the Italian Ministry for Education, University and Research (MIUR) for financial support within the "Futuro in Ricerca" (FIRB)

program (project DeLIGHTeD, Prot. RBFR12RS1W).

References

* Corresponding author: giorgio.pettinari@cnr.it

[1] S. Noda, Science **314**, 260 (2006).
[2] Y. Arakawa et al., IEEE J. Sel. Topics Quantum Electron. **18**, 1818 (2012).
[3] K. Hennessy et al., Nature **445**, 896 (2007).
[4] R. Trotta et al., Adv. Mater. **23**, 2706 (2011).
[5] S. Birindelli et al., Nano Lett. **14**, 1275 (2014).
[6] For a review, see G. Ciatto (ed.), Hydrogenated Dilute Nitride Semiconductors, Pan Stanford Publishing (2015).
[7] G. Pettinari et al., J. Appl. Phys. **115**, 012011 (2014); and references therein.
[8] E.M. Purcell, Phys. Rev. **69,** 681 (1946).
[9] A. Kaufman, Rev. Sci. Instrum. **61**, 230 (1990).
[10] R. J. Shul, and S. J. Pearton (Eds.), Handbook of Advanced Plasma Processing Techniques, Springer, Berlin (2000).
[11] G. J. Sonek and J. M. Ballantyne, J. Vac. Sci. Technol. B **2**, 653 (1984).
[12] K. J. Nordheden, D. W. Ferguson, and P. M. Smith, J. Vac. Sci. Technol. B **11**, 1879 (1993).
[13] D. F. Walls; G. G. J. Milburn (eds.), Quantum Optics, Springer: Berlin (2008).
[14] D. V. Regelman et al., Phys. Rev. Lett. **87**, 257401 (2001).
[15] T. Aichele, V. Zwiller, and O. Benson, New J. Phys. **6**, 90 (2004).
[16] P. Gallo et al., Appl. Phys. Lett. **92**, 263101 (2008).
[17] D. G. Gevaux et al., Appl. Phys. Lett. **88**, 131101 (2006).
[18] J. I. Pankove, Optical Processes in Semiconductors, Dover, New York (1975).
[19] M. Felici et al., in preparation (2016).
[20] H. Y. Liu et al., Appl. Phys. Lett. **83**, 4951 (2003).